HHS Public Access

Author manuscript

Nature. Author manuscript; available in PMC 2013 March 14.

Published in final edited form as:

Nature. 2008 November 27; 456(7221): 529–533. doi:10.1038/nature07476.

53BP1 facilitates long-range DNA end-joining during V(D)J recombination

Simone Difilippantonio[1], **Eric Gapud**[2], **Nancy Wong**[1], **Ching-Yu Huang**[2], **Grace Mahowald**[2], **Hua Tang Chen**[1], **Michael J. Kruhlak**[1], **Ferenc Livak**[3], **Michel Nussenzweig**[4,#], **Barry P. Sleckman**[2,#], and **André Nussenzweig**[1,#]

[1]Experimental Immunology Branch, National Cancer Institute, National Institutes of Health, Bethesda, Maryland 20892-1360

[2]Department of Pathology and Immunology, Washington University School of Medicine, St. Louis, Missouri 63110

[3]Department of Microbiology and Immunology, University of Maryland School of Medicine, Baltimore, Maryland 21201

[4]Laboratory of Molecular Immunology, The Rockefeller University and Howard Hughes Medical Institute, New York, New York 10021

Abstract

V(D)J recombination and class switch recombination employ overlapping but distinct non-homologous end-joining (NHEJ) pathways to repair DNA double strand break (DSB) intermediates. 53BP1 is a DNA damage response protein that is rapidly recruited to sites of chromosomal DSBs, where it appears to function in a subset of ataxia-telangiectasia mutated (ATM) kinase, H2AX- and MDC1- dependent events[1,2]. A 53BP1 dependent end joining pathway has been described that is dispensable for V(D)J recombination but essential for class-switch recombination CSR[3, 4]. Here, we report a previously unrecognized defect in the joining phase of V(D)J recombination in 53BP1 deficient lymphocytes distinct from that found in classical NHEJ-, *H2AX*-, *MDC1*- and *Atm*-deficient mice. Absence of 53BP1 leads to impairment of distal V-DJ joining with extensive degradation of un-repaired coding ends and episomal signal joint reintegration at V(D)J junctions. This results in apoptosis, loss of T-cell receptor alpha locus integrity and lymphopenia. Further impairment of the apoptotic checkpoint causes propagation of lymphocytes bearing antigen receptor breaks. These data suggest a more general role for 53BP1 in maintaining genomic stability during long range joining of DNA breaks.

RAG1 and RAG2 (RAG1/2) proteins perform the pair wise cleavage step in V(D)J recombination, whereas activation-induced cytidine deaminase (AID) triggers the formation of DSBs in the switch regions during CSR[5]. RAG1/2- and AID- induced lesions in antigen

Correspondence and requests for materials should be addressed to A.N. (andre_nussenzweig@nih.gov).

[#]These authors contributed equally

Supplementary Information is linked to the online version of the paper at www.nature.com/nature.

receptor loci initiate nuclear focus formation of the DNA damage response proteins γ-H2AX, NBS1 and 53BP1 over a large chromosome domain[5–8]. Based on the analysis of CSR in *H2AX*-[9], *Atm*-[7], and *53BP1*-deficient[3, 4, 10, 11] lymphocytes, it was proposed that focus forming factors might promote and/or maintain synapsis of distal switch regions[9]. In the case of *53BP1*-deficiency, there is an almost complete loss of long range CSR[3, 4, 12] and a concomitant increase in the frequency of short-range intra switch recombination[12]. Paradoxically, although V(D)J recombination and CSR employ similar DSB repair mechanisms, there are no known defects in V(D)J recombination in the absence of 53BP1[3, 4].

53BP1$^{-/-}$ mice show a 50–80% reduction in the number of B and T lineage cells, respectively, in bone-marrow and thymus (Supplementary Fig. 1a, b and [13]). This is similar to the lymphopenia found in *H2AX*$^{-/-}$, *MDC1*$^{-/-}$ and *Atm*$^{-/-}$ mice (Supplementary Fig. 1 and 2)[14, 15]. *Atm*$^{-/-}$ thymocytes express low levels of TCRαβ receptor, and we found a comparable defect in *53BP1*$^{-/-}$ but not in *H2AX*$^{-/-}$ or *MDC1*$^{-/-}$ thymocytes (Supplementary Fig. 1c; Supplementary Fig.2b). In addition, there was a reduction in the number of γ–δ T cells in the *53BP1*$^{-/-}$ thymus and spleen (Supplementary Fig. 1d), and a marked increase in apoptosis (Supplementary Fig. 1e). Transgenic expression of TCRαβ in the absence of endogenous recombination rescued the number of thymocytes to levels comparable to that of littermate controls (Supplementary Fig. 3), suggesting that decreased cellularity of the *53BP1*$^{-/-}$ thymus was due to defective V(D)J recombination.

To ascertain whether recombination defects exist in *53BP1*$^{-/-}$, *H2AX*$^{-/-}$ or *MDC1*$^{-/-}$ thymocytes, we initially assayed for TCRα locus integrity by 3 dimensional interphase DNA-FISH with 5’ and 3’ BAC probes (Fig. 1a)[16]. The probes were detected as two pairs of signals in the majority (>94 %) of *WT*, *H2AX*$^{-/-}$ and *MDC1*$^{-/-}$ thymocytes (Fig. 1a; Supplementary Fig. 2c). More rarely, *WT*, *H2AX*$^{-/-}$ and *MDC1*$^{-/-}$ thymocytes had either lost Cα (2 TCRVα, 1 TCRCα signal; up to 0.1 % of thymocytes) or both Vα and Cα from one allele (1 TCRVα, 1 TCRCα; up to 0.7% of thymocytes). In contrast to *H2AX*$^{-/-}$ and *MDC1*$^{-/-}$, *53BP1*$^{-/-}$ thymocytes exhibited a 7-fold increase in the number of aberrant cells (Fig. 1a; Supplementary Fig. 2c). Even when one TCR locus was entirely lost (1TCRVα, 1TCRCα), simultaneous hybridization with a centromeric chromosome 14 BAC probe confirmed that both chromosomes were present (data not shown), suggesting extensive but not complete chromosome 14 degradation (see below). Thus, 53BP1 is required for the stability of the TCRα locus, although the frequency of aberrant cells is higher in *Atm*$^{-/-}$ mice (Fig. 1a)[16].

To determine whether extensive thymocyte cell death or the stability of the TCRα locus is affected by pro-survival factors we bred *53BP1*-deficient mice with *p53*- deficient (*p53*$^{-/-}$) or mutant Nbs1 mice lacking the pro-apoptotic C-terminal portion of (*Nbs1*^{tr735})[17]. Although these crosses reduced the number of TUNEL positive thymocytes (Supplementary Fig. 1e, data not shown), they failed to rescue either the cellular or developmental defects associated with *53BP1*-deficiency (Supplementary Fig. 1a–d). However, further loss of the TCRα locus to levels approaching *Atm*-deficiency was found in double mutant *53BP1*$^{-/-}$*p53*$^{-/-}$ and *53BP1*$^{-/-}$*Nbs1*^{tr735} mice (Fig. 1a). Thus, although enhanced survival is insufficient to rescue lymphocyte development in *53BP1*$^{-/-}$ mice (Supplementary Fig. 1),

some of the *53BP1*$^{-/-}$ thymocytes that harbor un-repaired breaks in the TCR locus eventually die by a p53- and Nbs1-sensitive mechanism.

Our finding that loss of TCRα locus integrity is exacerbated in *53BP1*$^{-/-}$ thymocytes that are also *p53*- or *Nbs1*^{tr735}- deficient led us to investigate whether such cells would maintain V(D)J recombination induced chromosome aberrations in mature peripheral lymphocytes as previously shown in *Atm*$^{-/-}$ mice[8]. Whereas TCRα-associated chromosome breaks and translocations were undetectable or rare in metaphases from *WT* and *53BP1*$^{-/-}$ lymph node T cells, they were found in *53BP1*$^{-/-}$*p53*$^{-/-}$ and *53BP1*$^{-/-}$*Nbs1*^{tr735} doubly deficient mice at similar levels as seen in *Atm*$^{-/-}$ mice (Fig. 1b; Supplementary Table 1 and [8]). Likewise, concomitant loss of *p53* or the *Nbs1*-C terminus resulted in increased IgH-specific aberrations in *53BP1*$^{-/-}$ bone marrow, and these aberrations were maintained in the peripheral B cell compartment (Fig. 1c; Supplementary Table 1). We conclude that the long-term persistence of V(D)J recombination induced aberrations in *53BP1* knockout mice is limited by an intact apoptotic checkpoint.

Although antigen receptor associated DSBs occur in *53BP1*$^{-/-}$ lymphocytes (Fig. 1b, c), previous semi-quantitative analysis of TCRα rearrangements showed no defect[4]. However, measurement of recombination efficiency at this locus is complicated by the fact that there are multiple gene segments (100 Vα and 61 Jα), and TCRα alleles undergo primary and secondary rearrangements. To examine V(D)J recombination quantitatively, we evaluated rearrangements in mice homozygous for the *TCRα*^{SJ} allele, in which the 61 gene Jα cluster was replaced by 2 Jα segments[18] (Fig. 2a). Southern blot analysis of *TCRα*$^{SJ/SJ}$*:WT*, *TCRα*$^{SJ/SJ}$*:53BP1*$^{-/-}$, and *TCRα*$^{SJ/SJ}$*:Atm*$^{-/-}$ thymocyte DNA was used to assess aberrant Jα56 coding end accumulation. As previously documented, Jα56 coding ends accumulate as a discrete fragment in *TCRα*$^{SJ/SJ}$*:Atm*$^{-/-}$ but not in *TCRα*$^{SJ/SJ}$*:WT* thymocytes suggesting an end-joining defect in the absence of ATM[18] (Fig. 2a). Notably, multiple independent preparations of *TCRα*$^{SJ/SJ}$*:53BP1*$^{-/-}$ thymocytes displayed abnormal joining and coding end degradation, as evidenced by the CαI probe hybridizing with diffuse DNA fragments that migrated below the expected size of the Jα56 coding end (Fig. 2a). Furthermore, deoxynucleotidyl transferase (TdT) labeling of DNA ends revealed accumulation of the Jα coding ends and a broad smear of DNA that migrated below Jα61 in *TCRα*$^{SJ/SJ}$*:53BP1*$^{-/-}$ thymocytes (Fig. 2b,c). Taken together, these results suggest that in the absence of 53BP1 there is a repair defect and extensive nucleolytic processing of un-repaired V(D)J recombination induced coding ends.

To determine whether aberrant V(D)J recombination products were present in *53BP1* knockout thymocytes, we cloned and sequenced TCRβ, TCRα and TCRδ coding junctions (n=273) from *53BP1*$^{-/-}$ thymocytes. We found no statistically significant difference in the overall number of deletions or insertions at T-cell receptor loci (Supplementary Table 2). Furthermore, unlike classical NHEJ deficient mice, in which the majority of joins contain short stretches of homology indicative of an alternative end-joining mechanism[19], there was no bias in micro-homology joins in *53BP1*$^{-/-}$ mice (Supplementary Table 2). Nevertheless, four of the *53BP1*$^{-/-}$ junctions contained deletions >300 bp, four contained inserts >170 bp, and two of these junctions with insertions also showed significant degradation of V and J segments (Fig. 2d). In contrast, none of the 201 *WT* junctions analyzed showed such

abnormalities. Interestingly, the captured insertions in *53BP1*$^{-/-}$ junctions were not random, but were derived from intervening DNA that is normally deleted (Fig. 3d). This reintegration of excised episomes during V(D)J recombination constitutes a source of genome instability, and resembles the abnormalities reported for CSR junctions in *53BP1*$^{-/-}$ B cells[12].

Defective CSR in the absence of 53BP1 is associated with an increase in short-range intra switch recombination[12]. To determine whether 53BP1 facilitates joining of distal gene segments during V(D)J recombination, we performed quantitative PCR assays of partial (Dδ2-Jδ1 and Dδ1–Dδ2) and complete (Vδ5-Dδ1 and Vδ4-Dδ1) rearrangements. We found that short range (Dδ2-Jδ1 and Dδ1–Dδ2) rearrangements were similar to, or even more abundant in *53BP1*$^{-/-}$ than in *WT* thymocytes (Fig. 3a). In contrast, complete Vδ to DδJδ recombination was reduced approximately 2.5 fold in *53BP1* knockout thymocytes (Fig. 3a). To further substantiate these findings we compared Jα usage in *53BP1*$^{-/-}$ and *WT* thymocytes. Long range primary Vα-Jα rearrangements (involving at least 200 kb) use Jα segments at the 5' end of the Jα array and these are replaced by shorter-range secondary rearrangements that use progressively more 3' segments at the end of the Jα locus. Comparison of Jα usage in *53BP1*$^{-/-}$ and *WT* thymocytes revealed that the 5' proximal Jα segments were under-represented in *53BP1*$^{-/-}$ mice by at least 2-fold while distal ones were relatively increased (Supplementary Fig. 4). Taken together, these data suggest that long-range V(D)J recombination is impaired in *53BP1* knockout mice whereas short-range recombination is not affected and may be favored.

If distal joining were preferentially impaired, we would expect that the distances separating the TCR Vα and Jα segments would be greater in the absence of 53BP1. To study the compaction state of the TCRα locus, we measured distances between 5' Vα and 3' Cα probes in CD4^{+}CD8^{+} double positive (DP) thymocytes that are actively undergoing TCRα recombination (Fig. 3b). Three different 5' and 3' BAC probe sets separated by 0.820 Mb (proximal), 1.6 Mb (middle) and 2.1 Mb (distal) were used to map spatial distances along the TCRα locus (Fig. 3b). The average distance (D) between proximal probes (334B8-255N13) was similar in WT (D=0.216 μM) and *53BP1*$^{-/-}$ DP thymocytes (D=0.225 μM, WT vs. *53BP1*$^{-/-}$, p=0.57, two-tailed Wilcoxon rank sum test), and 81–83% of the alleles were separated by distances of less than 0.3 μM in both cases (Fig. 3b, Supplementary Table 3, and Supplementary Fig. 5). In contrast, the distribution of distances amongst intact TCRα alleles in *53BP1*$^{-/-}$ DP thymocytes was substantially shifted towards larger separations when assessed using either middle (74E19-17317) or distal (304L21-10K20) probe sets (Fig. 3b, Supplementary Table 3, and Supplementary Fig. 5). For example, the average distance between the 5' and 3' ends of the TCRα locus was 1.4-fold greater in *53BP1*$^{-/-}$ compared to *WT* DP thymocytes (Fig. 3b; middle probes, WT: D= 0.273 μM; *53BP1*$^{-/-}$: D=0.396 μM, p<0.0001;distal probes, WT: D=0.287 μM; *53BP1*$^{-/-}$: D=0.426 μM, p<0.0001). In *53BP1*$^{-/-}$ DP thymocytes, middle and distal genes were separated by 0.5–2 μM in 23–32% of nuclei compared to only 7–9% in WT. In contrast to DP thymocytes, the distribution of spatial distances was similar for loci not undergoing recombination (chromosome band 1D and the TCRα locus in CD4$^{-/-}$CD8$^{-/-}$ (DN) thymoctyes; Fig. 3b and Supplementary Table 3). We conclude that the distal portion of the TCRα locus is in a more extended state in *53BP1*$^{-/-}$ DP thymocytes.

RAG1/2 initiates recombination by binding to a single recombination signal sequence (RSS) and introduces a lesion in the target DNA[20,21] (Fig 4, steps 1, 2). It is believed that a synaptic complex is produced when a second RSS is captured[20, 21]. 53BP1 interacts constitutively with chromatin in the absence of DNA damage via its methyl-histone binding Tudor domain[22,23,24]. 53BP1 oligomerization[25] may promote a basal level of RSS synapsis by increasing the effective local concentration of the RSSs, thereby promoting their pairing (Fig. 4, steps 1, 2). 53BP1 has also been reported to interact with motor proteins[26], which may enhance chromatin mobility. Upon DNA damage the affinity of 53BP1 for DNA is increased by mechanisms that involve interaction with H2AX and MDC1[1, 2, 24]. We speculate that the initiating lesions in V(D)J recombination promote high affinity binding of 53BP1, and that this further amplifies 53BP1 homo-oligomerization and therefore the efficiency of long-range synapsis (Fig. 4, step 3). 53BP1 recruitment to DSB-flanking chromatin could also serve an important role in the post-cleavage phase of the recombination reaction by protecting coding ends from premature release from the synaptic complex and from degradation before the breaks are repaired by NHEJ (Fig. 4, steps 4 and 5). Similarly, joining of distal switch regions during CSR would be favored by high affinity binding of 53BP1 and local chromatin contraction to bring together damaged DNA ends[3, 4,10–12].

Such a model would be compatible with the NHEJ defect in the absence of 53BP1 due to loss of both “basal” and DNA damage induced RSS tethering, and with the mild joining defect in the absence of H2AX or MDC1, where only the DSB induced amplification of 53BP1’s affinity for damaged chromatin is impaired. We propose that 53BP1-mediated chromosome tethering and/or mobility evolved to facilitate chromosomal end-joining, and thereby favor long-range interactions between DNA ends that have an otherwise low probability of encountering each other[27].

Online Methods

Metaphase and interphase FISH

Metaphase spreads from cultured lymphocytes were prepared and analyzed by FISH[8] using BAC probes containing the TCRα locus (TCR Cα-17317 and TCR Vα-RP24-74E19), the IgH locus (IgH Vα-224M14), IgH Cα (from Cγ1- 3’of Cα) and a telomere-repeat specific peptide nucleic acid (PNA) probe (Applied Biosystems). Three dimensional FISH on freshly isolated thymocytes using TCRvα and TCRcα locus specific probes was performed as described[8]. Confocal image stacks were collected using a Zeiss LSM510 META microscope equipped with a 63× Plan-Apochromat (N.A. 1.4) objective lens with 0.07μm X-Y pixel sampling, optical slice thickness of 0.8μm, and Z-step size of 0.2μm. Volumes of interest (VOIs) were drawn around FISH spots to be measured. Within the individual VOIs, the center of intensity mass was calculated for each FISH spot and the 3-dimensional distance between red and green spots was measured using customized software (MIPAV, CIT/NIH). Tetraspeck fluorescent microspheres (Molecular Probes/Invitrogen) 0.1μm and 0.5μm in diameter were imaged using the same microscope parameters and used to model the point spread function of the microscope, fluorescence channel alignment, and to determine the validity of the MIPAV software to accurately measure the center of intensity mass of a

fluorescence object. The minimum measurable distance between the two fluorescence points was 70nm in the lateral dimension. For distance measurements the following TCRα probe sets were used: RP24-334B8 and RP23-255N13 (proximal), RP24-74E19 and 17317 (middle), RP23-304L21 and RP23-10K20 (distal) and as control RP23-309A8 and RP24-336F10 which are separated by 1 Mb and map to mouse chromosome 1D.

Flow cytometry

Thymocytes were washed twice in HBSS containing 0.1% BSA and 0.1% NaN_3 and stained with antibodies specific for CD4, CD8, TCRβ (H57-597), TCR γδ (GL3) (BD PharMingen, San Diego, CA).

PCR and junction analysis

Genomic DNA was isolated from thymocytes using a QIAGEN DNA isolation kit (QIAGEN, Valencia, CA). 50ng DNA was PCR amplified with a combination of gene-specific primers (Supplementary Table 3) using Platinum Taq polymerase (Invitrogen, Carlsbad, CA) for standard, or the Power Sybr Green™ Master Mix kit (Applied Biosystems, Foster City, CA) for qPCR. Real-time qPCR was performed in duplicate and data were collected on an ABI 9700 Sequence Analyzer and analyzed using the SDS 2.2 software (Applied Biosystems, Foster City, CA). For each assay, aliquots of DNA were analyzed for a control, non-rearranging DNA 3' of Jδ2. The cycle threshold numbers for each primer combinations (C_t^{exp}) and for the control amplification (C_t^{ctr}) were used to calculate the absolute amount of PCR signal. The relative ratios of each rearrangement were averaged and plotted together with the standard error of the mean. For sequence analysis, 150 ng of thymocyte DNA was used to amplify coding joints which were cloned using a TA cloning kit (Invitrogen). Primers for TCRβ coding joints were published[28]. To PCR amplify TCR V-DJδ coding joint sequences, Vδ primers were used as forward primers with the primer 3Jδ1 as reverse primer (Supplementary Table 4). Junctions from $TCR\alpha^{SJ}$ mice were amplified using the indicated primers (Supplementary Table 4). TCR Jα usage was determined as previously described[29].

Southern blot analysis

Southern blot analysis was carried out as previously described[18]. Briefly, 10 μg of total thymus genomic DNA was digested with Stu*I* (New England Biolabs). The digest products were run out on a 1% agarose TAE gel, transferred onto Zeta-Probe GT membrane and probed with the Cα-I for coding joints and coding ends. The same membrane was stripped and reprobed with RAG2 as a loading control.

TdT-mediated polyadenylation and PCR amplification of free Jα coding ends

One μg of genomic DNA was treated with terminal deoxynucleotidyl transferase (New England Biolabs) per manufacturer's protocol at a final concentration of 5μM dATP. Terminal deoxynucleotidyl transferase was subsequently terminated by heating to 70°C for 15 minutes. Two percent of the total volume of each poly-adenylation reaction was then used for primary amplification using D1 and T17-UNIV primers. Conditions were 95°C for 5 minutes followed by 15 cycles of 95°C for 1 minute, 57°C for 45 seconds, and 72°C for 45

seconds and then a final 5 minute extension step at 72°C. Two percent by volume of each primary amplification reaction was then serially diluted 5-fold in water. One μl of the original primary reaction and of each serial dilution were used as template for a secondary amplification step using primers D2 and UNIV-BglII. Reaction conditions were the same as for the primary reactions, but the total number of cycles was increased to 30 cycles total. 15μl of each secondary reaction was run out on a 1% agarose TBE gel and then transferred onto Zeta-Probe GT membrane (Bio-Rad). The membrane was subsequently hybridized with ^{32}P-labeled DS850 oligonucleotide. For IL-2 loading control PCR reactions, aliquots of the DNA samples used for poly-adenylation were serially diluted 5-fold and amplified as previously described[30]. 10μL of each PCR product was run out on a 1% agarose TBE gel and then transferred overnight onto Zeta-Probe GT membrane (Bio-Rad). The oligonucleotides D1, D2, UNIV-BglII, T17-UNIV and DS850 are listed in Supplementary Table 4.

TUNEL staining

Thymi were fixed in buffered 10% formalin, and paraffin sections were stained with hematoxylin-eosin. Apoptotic nuclei were detected with TdT-mediated dUTP-biotin nick labeling.

Supplementary Material

Refer to Web version on PubMed Central for supplementary material.

Acknowledgements

We are grateful to Matt McAuliffe and coworkers (Biomedical Imaging Research Services Section BIRSS/CIT/NIH) for developing the 3D-FISH measurement algorithm; David G. Schatz (Yale University) and Jim Haber (Brandeis University) for helpful discussions; A.Wynshaw-Boris (UCSD) for *Atm*$^{-/-}$ mice and Junjie Chen (Yale University) for *53BP1*$^{-/-}$ and *MDC1*−/− mice; D. Venzon for help with statistical analysis; and members of the A. Nussenzweig lab (Jeremy Daniel, Elsa Callen, and Arkady Celeste) for comments on the manuscript. B.P. S. is supported by NIH grant R01AI074953. E. G. is supported by pre-doctoral fellowship from the Cancer Research Institute. M.C.N. is a HHMI investigator. A.N. is supported by the Intramural Research Program of the NIH, National Cancer Institute, Center for Cancer Research.

References

1. Stucki M, Jackson SP. gammaH2AX and MDC1: anchoring the DNA-damage-response machinery to broken chromosomes. DNA repair. 2006; 5:534–543. [PubMed: 16531125]
2. Fernandez-Capetillo O, Lee A, Nussenzweig M, Nussenzweig A. H2AX: the histone guardian of the genome. DNA repair. 2004; 3:959–967. [PubMed: 15279782]
3. Manis JP, et al. 53BP1 links DNA damage-response pathways to immunoglobulin heavy chain class-switch recombination. Nature immunology. 2004; 5:481–487. [PubMed: 15077110]
4. Ward IM, et al. 53BP1 is required for class switch recombination. The Journal of cell biology. 2004; 165:459–464. [PubMed: 15159415]
5. Petersen S, et al. AID is required to initiate Nbs1/gamma-H2AX focus formation and mutations at sites of class switching. Nature. 2001; 414:660–665. [PubMed: 11740565]
6. Chen HT, et al. Response to RAG-mediated VDJ cleavage by NBS1 and gamma-H2AX. Science (New York, N.Y. 2000; 290:1962–1965.
7. Reina-San-Martin B, Chen HT, Nussenzweig A, Nussenzweig MC. ATM is required for efficient recombination between immunoglobulin switch regions. The Journal of experimental medicine. 2004; 200:1103–1110. [PubMed: 15520243]

8. Callen E, et al. ATM prevents the persistence and propagation of chromosome breaks in lymphocytes. Cell. 2007; 130:63–75. [PubMed: 17599403]
9. Reina-San-Martin B, et al. H2AX is required for recombination between immunoglobulin switch regions but not for intra-switch region recombination or somatic hypermutation. The Journal of experimental medicine. 2003; 197:1767–1778. [PubMed: 12810694]
10. Ramiro AR, et al. Role of genomic instability and p53 in AID-induced c-myc-Igh translocations. Nature. 2006; 440:105–109. [PubMed: 16400328]
11. Franco S, et al. H2AX prevents DNA breaks from progressing to chromosome breaks and translocations. Molecular cell. 2006; 21:201–214. [PubMed: 16427010]
12. Reina-San-Martin B, Chen J, Nussenzweig A, Nussenzweig MC. Enhanced intra-switch region recombination during immunoglobulin class switch recombination in 53BP1−/− B cells. European journal of immunology. 2007; 37:235–239. [PubMed: 17183606]
13. Ward IM, Minn K, van Deursen J, Chen J. p53 Binding protein 53BP1 is required for DNA damage responses and tumor suppression in mice. Molecular and cellular biology. 2003; 23:2556–2563. [PubMed: 12640136]
14. Celeste A, et al. Genomic instability in mice lacking histone H2AX. Science (New York, N.Y. 2002; 296:922–927.
15. Lou Z, et al. MDC1 maintains genomic stability by participating in the amplification of ATM-dependent DNA damage signals. Molecular cell. 2006; 21:187–200. [PubMed: 16427009]
16. Matei IR, et al. ATM deficiency disrupts Tcra locus integrity and the maturation of CD4+CD8+ thymocytes. Blood. 2007; 109:1887–1896. [PubMed: 17077325]
17. Difilippantonio S, et al. Distinct domains in Nbs1 regulate irradiation-induced checkpoints and apoptosis. The Journal of experimental medicine. 2007; 204:1003–1011. [PubMed: 17485521]
18. Huang CY, et al. Defects in coding joint formation in vivo in developing ATM-deficient B and T lymphocytes. The Journal of experimental medicine. 2007; 204:1371–1381. [PubMed: 17502661]
19. Gu Y, et al. Growth retardation and leaky SCID phenotype of Ku70-deficient mice. Immunity. 1997; 7:653–665. [PubMed: 9390689]
20. Curry JD, Geier JK, Schlissel MS. Single-strand recombination signal sequence nicks in vivo: evidence for a capture model of synapsis. Nature immunology. 2005; 6:1272–1279. [PubMed: 16286921]
21. Jones JM, Gellert M. Ordered assembly of the V(D)J synaptic complex ensures accurate recombination. The EMBO journal. 2002; 21:4162–4171. [PubMed: 12145216]
22. Huyen Y, et al. Methylated lysine 79 of histone H3 targets 53BP1 to DNA double-strand breaks. Nature. 2004; 432:406–411. [PubMed: 15525939]
23. Botuyan MV, et al. Structural basis for the methylation state-specific recognition of histone H4-K20 by 53BP1 and Crb2 in DNA repair. Cell. 2006; 127:1361–1373. [PubMed: 17190600]
24. Bekker-Jensen S, Lukas C, Melander F, Bartek J, Lukas J. Dynamic assembly and sustained retention of 53BP1 at the sites of DNA damage are controlled by Mdc1/NFBD1. The Journal of cell biology. 2005; 170:201–211. [PubMed: 16009723]
25. Adams MM, et al. 53BP1 oligomerization is independent of its methylation by PRMT1. Cell cycle (Georgetown, Tex. 2005; 4:1854–1861.
26. Lo KW, et al. The 8-kDa dynein light chain binds to p53-binding protein 1 and mediates DNA damage-induced p53 nuclear accumulation. The Journal of biological chemistry. 2005; 280:8172–8179. [PubMed: 15611139]
27. Jhunjhunwala S, et al. The 3D structure of the immunoglobulin heavy-chain locus: implications for long-range genomic interactions. Cell. 2008; 133:265–279. [PubMed: 18423198]
28. Talukder SR, Dudley DD, Alt FW, Takahama Y, Akamatsu Y. Increased frequency of aberrant V(D)J recombination products in core RAG-expressing mice. Nucleic acids research. 2004; 32:4539–4549. [PubMed: 15328366]
29. Huang CY, Sleckman BP. Developmental stage-specific regulation of TCR-alpha-chain gene assembly by intrinsic features of the TEA promoter. J Immunol. 2007; 179:449–454. [PubMed: 17579065]

30. Bredemeyer AL, et al. ATM stabilizes DNA double-strand-break complexes during V(D)J recombination. Nature. 2006; 442:466–470. [PubMed: 16799570]

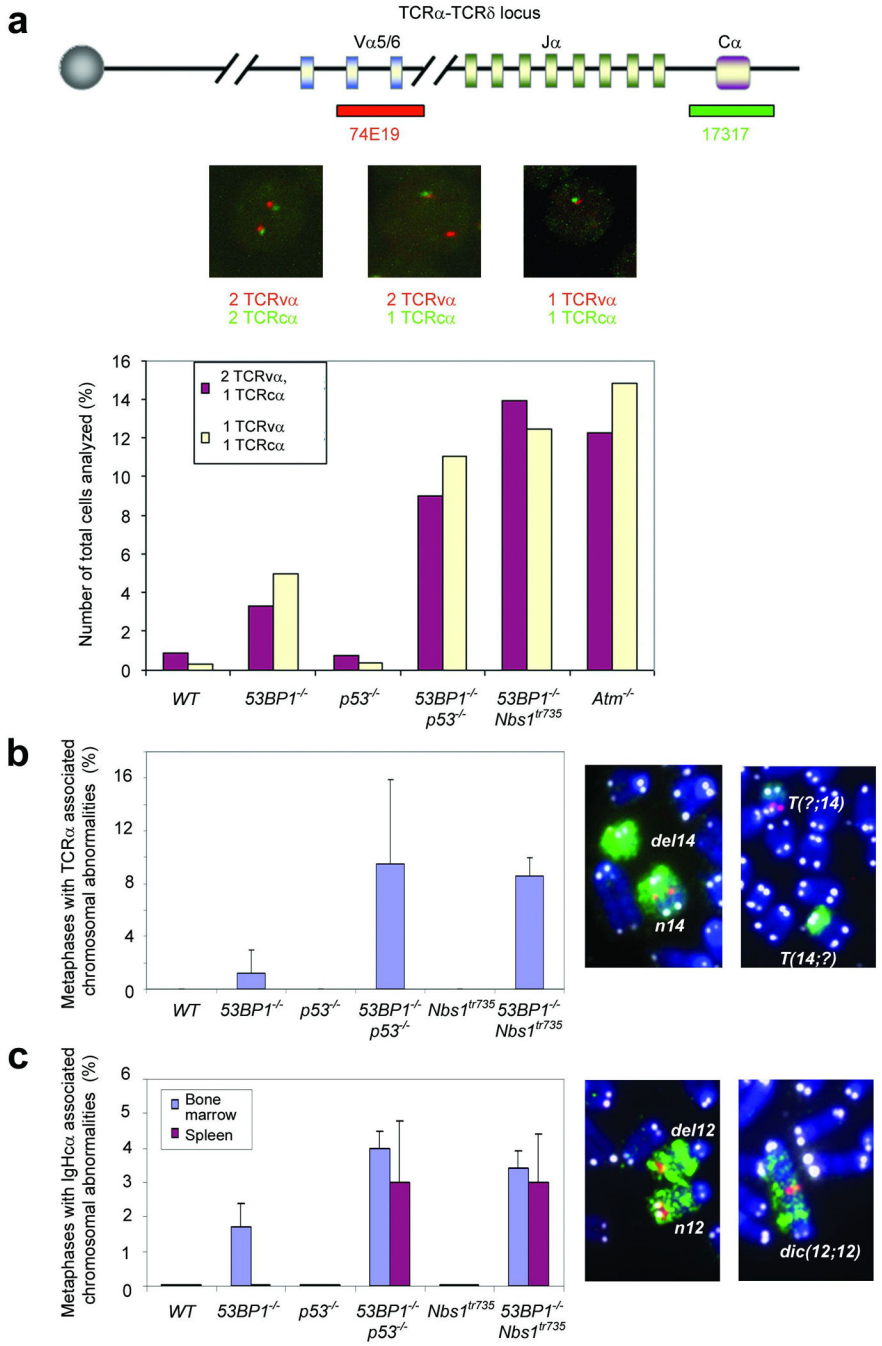

Figure 1. Antigen-receptor-associated aberrations in *53BP1*$^{-/-}$ lymphocytes

a, Upper panel: schematic of the TCRα-TCRδ locus with positions of the BACs used for generation of DNA-FISH probes indicated. Middle panel: Representative examples of projections of confocal sections, analyzed by three-dimensional FISH on freshly isolated thymocytes. Bottom panel: frequency at which TCRcα or (TCRvα+ TCRcα) signal is lost from one allele in *WT*, *53BP1*$^{-/-}$, *p53*$^{-/-}$, *53BP1*$^{-/-}$*p53*$^{-/-}$, *53BP1*$^{-/-}$*Nbs1*^{tr735} and *Atm*$^{-/-}$ thymocytes (>200 cells analyzed per genotype in each of two experiments;error bars, s.d.). **b**, TCRα associated chromosomal aberrations in lymph node T cells determined by FISH

using a TCRα locus spanning BAC (red signal, right panel), a chromosome 14 paint (green signal, right panel) and a telomere repeat specific probe (white signal, right panel). T cells were stimulated with anti-TCR/CD28 antibodies for 48 hours. (error bars, s.d., n≥3).**c**, Frequency of IgH-associated abnormalities in metaphase spreads from bone marrow and splenic B cells from *WT*, *53BP1*$^{-/-}$, *53BP1*$^{-/-}$*p53*$^{-/-}$ and *53BP1*$^{-/-}$*Nbs1*^{tr735} mice (error bars, s.d., n≥3). B220^{+} bone marrow cells were cultured on irradiated S17 stromal cells in the presence of IL7 for 5 days. Splenic CD43-negative B cells were cultured for 1 day with RP105, which induces proliferation but not CSR[8]. FISH was performed using probes specific for the IgHcα locus (red signal, right panel), chromosome 12 (green signal, right panel) and telomeric repeats (white signal, right panel).

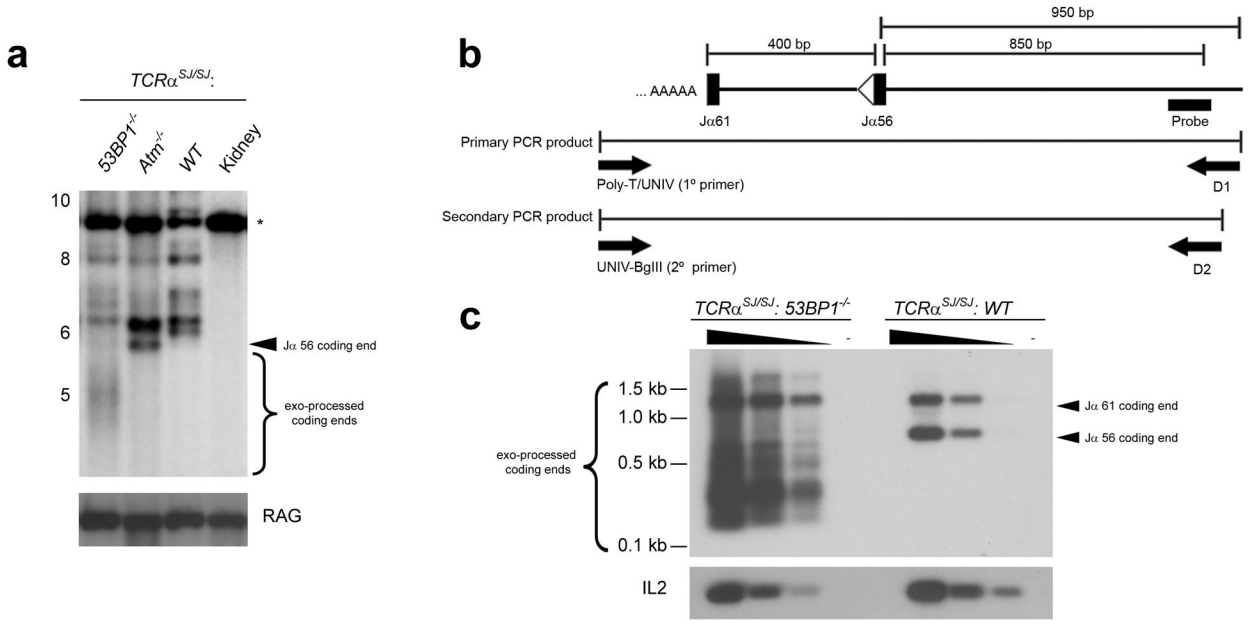

d

	Vα	P/N	Jα56
	gagactcagccacctacttctgtgcagcaagtg		**tggctactggaggcaataataagctgacttttggtc**
WT	gagactcagccacctacttctgtgcagcaag	GG	ggctactggaggcaataataagctgacttttggtc
53BP1$^{-/-}$	gagactcagccacctacttctgtgcagcaagtg	200 bp insert[a]	gaggcaataataagctgacttttggtc

	Vδ2	P/N	Dδ1	P/N	Dδ2	P/N	Jδ1
	ctcaggcacttacctctgtggagggaaag		**gtggcatat**		**atcggagggatacgag**		**taccgacaaactcgtctttgg**
WT	ctcaggcacttacctctgtggagggaaag	GT	atat	T	tcggagggatacgag	CTAC	ccgacaaactcgtctttgg
53BP1$^{-/-}$	ctcaggcacttacctctgtggagggaaag	294 bp insert[b]			cggagggatac	AATAGC	taccgacaaactcgtctttgg
53BP1$^{-/-}$	-389 bp	170 bp insert[c]					ctttgg
53BP1$^{-/-}$	-554 bp	383 bp insert[d]					taccgacaaactcgtctttgg

	Vδ3	P/N	Dδ1	P/N	Dδ2	P/N	Jδ1
	tgtgtaccactgtatcctgagagtag		**gtggcatat**		**atcggagggatacgag**		**taccgacaaactcgtctttgg**
WT	tgtgtaccactgtatcctgagagtag	CA	ggcatat	GAGGAT	atcggagggata	AAGC	taccgacaaactcgtctttgg
53BP1$^{-/-}$	-374 bp			TA	cg	GGC	taccgacaaactcgtctttgg
53BP1$^{-/-}$	-519bp		gtggcat		atcggaggg	GCAGTTC	taccgacaaactcgtctttgg

Figure 2. Processing of Jα coding ends in 53BP1 deficient thymocytes

a, Southern blot analysis of total thymocyte and kidney DNA digested with Stu*I* and hybridized with a CαI probe. The same blot was stripped and re-probed with a RAG2 probe as a loading control. The fragments corresponding to the germline *TCRα*^{SJ} allele (*) allele, the Jα56 coding ends, as well as the molecular mass markers (in kb) are indicated. **b**, Strategy for PCR amplification of free Jα coding ends captured by TdT-mediated poly-adenylation. **c**, Southern blot analysis of coding ends from *TCRα*$^{SJ/SJ}$*:WT* and *TCRα*$^{SJ/SJ}$*: 53BP1*$^{-/-}$ thymocytes. Serial five-fold dilutions and a mock-polyadenylated control are shown. IL-2 gene PCR templated with serial five-fold dilutions of the genomic DNA used for polyadenylation is shown as a loading control. **d**, Examples of sequences of coding joints formed by V(D)J recombination. Germline coding sequences (bold face lowercase letters) are indicated on the top. Nucleotide insertions (P/N) are indicated by capital letters. Sequences of inserts[a–d] are listed in Supplementary Table 2.

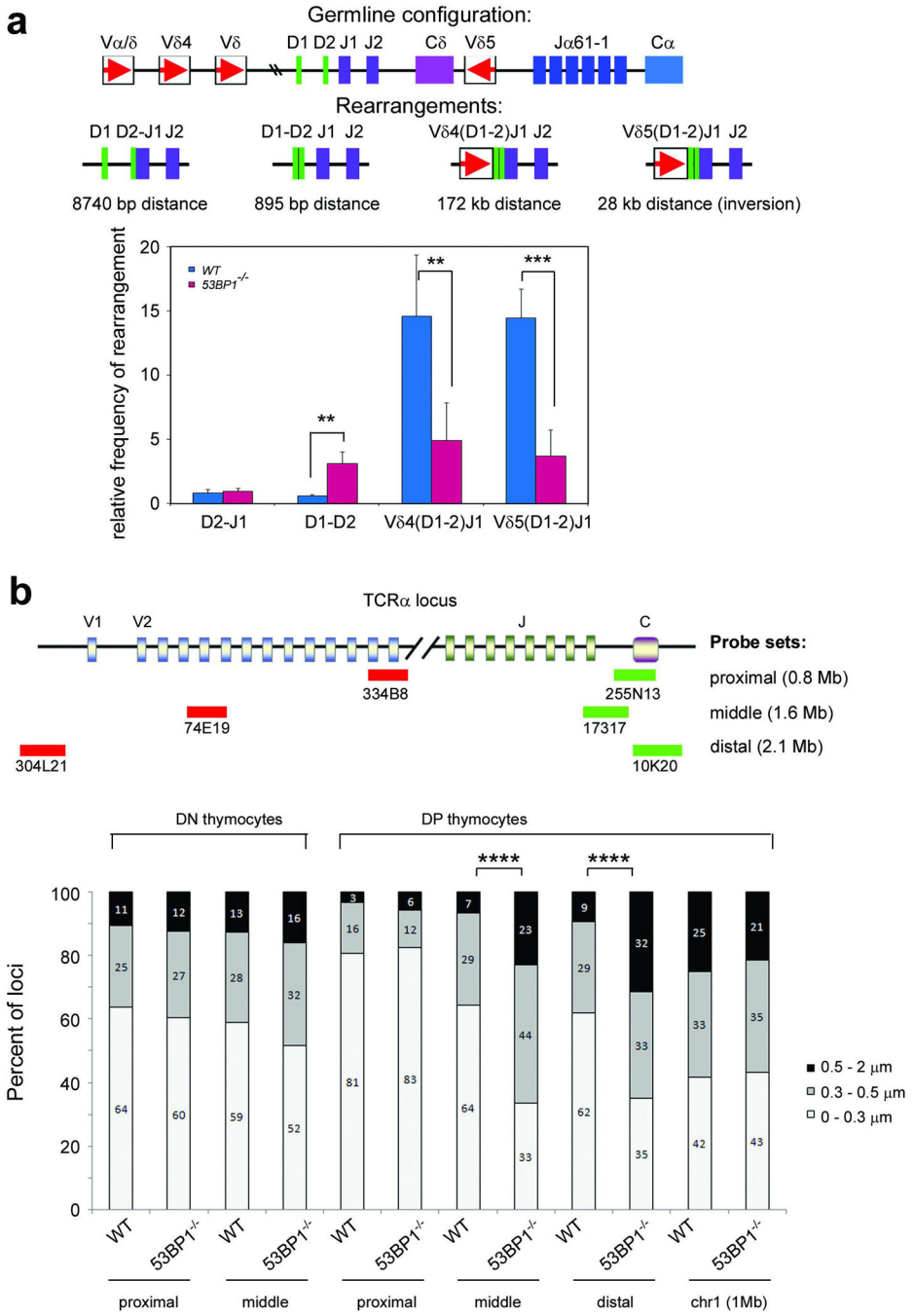

Figure 3. Decreased efficiency of long-range VDJ recombination and TCRα locus contraction in *53BP1*$^{-/-}$ thymocytes

a, Schematic of the mouse TCRα/δ locus is shown in the top panel with the four different TCRδ rearrangements depicted individually below. Frequency of TCRδ locus rearrangements in total thymocytes from *53BP1*$^{-/-}$ and *WT* littermates. Quantitative assessment of genomic DNA rearrangements of Dδ1 to Dδ2, Dδ2 to Jδ1, and Vδ4 and Vδ5 to (D)Jδ1 genes were performed by quantitative PCR and normalized to the signal of the non-rearranging DNA 3' of Jδ2. Results are averaged from 4 *53BP1*$^{-/-}$ and 2 *WT* mice with

duplicate measurements, and standard errors of the mean are shown. (WT vs. *53BP1*$^{-/-}$: D2-J1, p=0.851; D1–D2, p=0.001;V4-DJ1, p=0.003; V5-DJ1, p<0.001). **b**, Distances separating the TCRVα and TCRCα loci in freshly isolated CD4/CD8 double negative (DN) or double positive (DP) thymocytes. The data were obtained by three-dimensional DNA-FISH using the TCRα BAC probes as indicated (top panel). As control, the probe set RP23-309A8 and RP24-336F10 (1Mb distance) on mouse chromosome 1D was used. Light grey bars: 0 to 0.3 μm; dark grey bars: 0.3–0.5 μm and black bars: 0.5 to 2 μm. Distance distribution histograms are shown in Supplementary Fig. 4, and Supplementary Table 3 lists sample sizes and average distances. (error bars, s.d.; *****: p<0.0001).

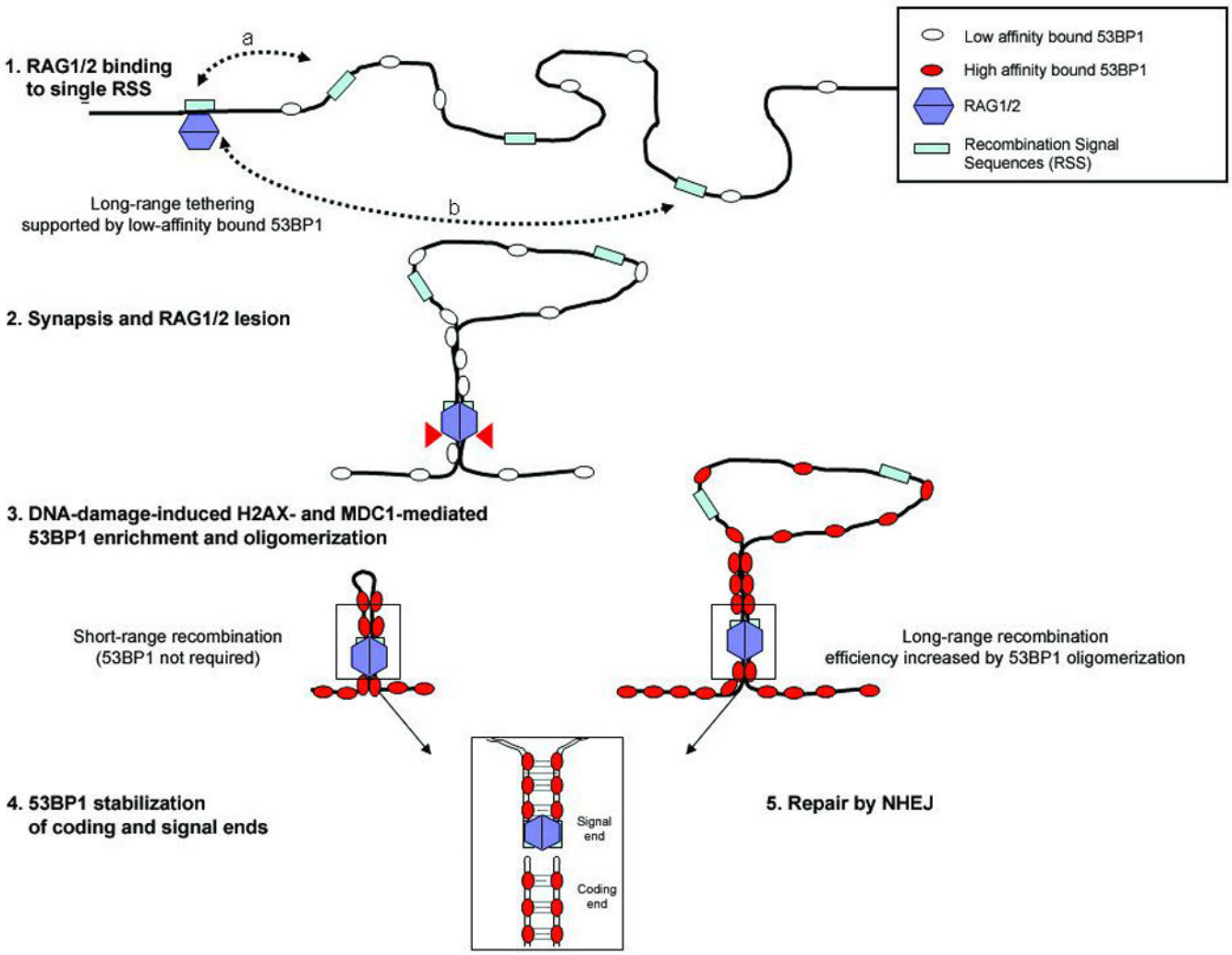

Figure 4. Model for 53BP1's role in promoting and/or maintaining synapsis during V(D)J recombination

Before recombination, 53BP1 is loosely associated with chromatin (Step 1). RSS's that are at a close physical distance (a) spend more time near the RAG1/2- bound RSS than distant RSS's (b), and have a high probability of synapsis whether or not 53BP1 is present. 53BP1 homo-oligomerization increases the effective local concentration of distant RSSs thereby promoting their pairing. When RAG1/2 associates with and cleaves a single RSS, 53BP1 accumulates at the lesion and binds tightly to flanking chromatin in a manner dependent on H2AX and MDC1 (Steps 2 and 3). After RAG1/2 mediated DSB formation (step 4), 53BP1 stabilizes the post-cleavage complex, thereby increasing the efficiency of non-homologous end-joining (Step 5).